Eur. Phys. J. B **30**, 581–585 (2002)
DOI: 10.1140/epjb/e2002-00417-1

THE EUROPEAN PHYSICAL JOURNAL B

# Self-averaging in complex brain neuron signals

A. Bershadskii[1,a], E. Dremencov[2], D. Fukayama[3], and G. Yadid[2]

[1] ICAR, PO Box 31155, Jerusalem 91000, Israel
and
Kavli Institute for Theoretical Physics, University of California, Santa Barbara, California 93106-4030, USA
[2] Faculty of Life Sciences, Bar-Ilan University, Ramat-Gan 52900, Israel
[3] Information and Mathematical Science Laboratory Inc. 2-43-1, Ikebukuro, Toshima-ku, Tokyo, 171-0014, Japan

Received 17 April 2002 / Received in final form 30 September 2002
Published online 31 December 2002 – 

**Abstract.** Nonlinear statistical properties of Ventral Tegmental Area (VTA) of limbic brain are studied *in vivo*. VTA plays key role in generation of pleasure and in development of psychological drug addiction. It is shown that spiking time-series of the VTA dopaminergic neurons exhibit long-range correlations with self-averaging behavior. This specific VTA phenomenon has no relation to VTA rewarding function. Last result reveals complex role of VTA in limbic brain.

**PACS.** 87.19.La Neuroscience – 87.18.Sn Neural networks – 87.17.-d Cellular structure and processes – 87.10.+e General theory and mathematical aspects

## 1 Introduction

Methods of statistical physics are actively used for investigation of probabilistic properties of neurons [1–12]. In papers [9,12] we studied probabilistic properties of spiking time-series in the Red Nucleus of brain. It is believed that the Red Nucleus is mainly responsible for motor activity and, therefore, is relatively simple [13]. In the present paper we will study the data obtained *in vivo* for so-called Ventral Tegmental Area (VTA).

The Ventral Tegmental Area (VTA) is a midbrain nucleus consisting of the dopaminergic cells. VTA is known as a part of limbic brain that corresponds to such high brain functions as cognition, learning, rewarding and emotional behavior. VTA plays key role in the generation of pleasure and in development of psychological drug addiction. This area is also involved in control of the gonadal hormones and of the reinforcement behavior [13].

The VTA dopaminergic cells fire in irregular manner with a mean rare rate between 0.5 to 10 Hz. Firing patterns of the VTA dopaminergic cells include single spikes and short bursts containing 3−7 spikes. It is believed that the bursting manner of firing is probably pulled on by rewarding stimuli accepted from the glutamate neurons originating from prefrontal cortex and hippocampus. Bursting activity of the normal VTA dopaminergic cells results in dopamine release in limbic brain. Dopamine release from VTA dopaminergic cells accompanies rewarding behavior. VTA dopaminergic cells are autoregulated *via* dopamine autoreceptors expressed on their somas. Additionally, activity of the VTA dopaminergic cells is regulated by serotonin, noradrenaline and acetylcholine.

Specific nonlinear properties of the VTA dopaminergic neurons are actively studied in recent years (see, for instance [4,5] and references therein). Relationship between these properties and rewarding function of VTA is one of the topical problems. Therefore, comparative analysis of the nonlinear properties of the VTA signals generated by normal brains and ones generated by brains with genetically suppressed rewarding function of VTA seems to be of significant interest. For this purpose we use genetically defined rat model of depression (Flinders Sensitive Rat Line – FSL).

It is shown in [9] that probability distribution of the interspike intervals in Red Nucleus can be used to distinguish between normal rats and genetically defined rat model of depression (FSL). It is shown below that probability distributions of the interspike intervals in FSL VTA are significantly different from those in VTA of normal rates. In VTA, similarly to Red Nucleus, these differences can be related to the underlying kinetic problems of *individual* neurons rather than to *system* behavior.

On the other hand, it is shown in paper [12] that the spiking time-series of Red Nucleus neurons exhibit multifractal properties (related to system behavior), which are generally the same for the normal and for the FSL brains. We will show below that the spiking time-series of the VTA neurons also exhibit multifractal properties both for normal and for FSL brains. The VTA multifractality is different from multifractality of Red Nucleus. This

[a] e-mail: ark2@eudoramail.com

difference between the long-range correlations in the Red Nucleus and the VTA signals is then explained in the terms of a self-averaging processes in the VTA signals. The self-averaging phenomenon is observed for both the FSL and the normal rats. Therefore, this phenomenon is independent on rewarding function of VTA. This observation shows that the main differences between Red Nucleus and VTA at system level cannot be reduced to rewarding function of VTA.

## 2 Experimental methods and materials

Male Sprague-Dawley tars were used in all experiments. Animals were anaethtised with chloral hydrate (400 mg/kg., i.p.) and mounted in stereotaxic apparatus. The hole was drilled 4.2 mm. anterior from the interaural line and 1.0 mm lateral from the medial line. Extracellular recordings were processed by an electrode from VTA (8.0−8.6 mm dorsal from the lambda). The constant level of the anaesthesia was checked by EKG and chloral hydrate was added as necessary. Single unit recording was carried out by amplitude discrimination. Each recording from the single cell included at least 2000 spike events. After each experiment, the recording site was marked by a lesion caused by 15 mA DC for 10 sec. Brains were removed and stained with formalin before histological examination. Frozen sections were cut at 50 mm intervals. Microscopic examination of the sections was carried out aiming to verify that the electrode tip was placed in VTA.

## 3 Short-range correlations

Figure 1 (a, b and c) shows probability density functions of interspike intervals, $P(\tau)$. $P(\tau)$ were calculated using data from three dopaminergic neurons in VTA of the FSL rats (length of interspike intervals, $\tau$, is given in seconds). Solid curves (best fit) in this figure indicate lognormal distribution.

Figure 2 (a, b and c) shows the probability density functions for three dopaminergic neurons in VTA area of the rats from control (healthy) group. Since we choose log-log scales the straight lines (best fit) indicate power-law distribution in this figure. In Figures 2b and c one can also see a sharp transition at $\tau \simeq 0.7$ s from a power-law distribution to a lognormal-like tale (bell shaped in the log-log scales).

It is interesting that the data, obtained from the *ill* dopaminergic neurons, can be fitted by the same (lognormal) probability distribution, as for the healthy *non*-dopaminergic neurons, (*i.e.* for Red Nucleus, see [9] and references therein). This may mean that in the ill state the dopaminergic neurons lose their specific electrochemical properties which distinguish them from other types of neurons. It should be noted that in the ill state they also stop dopamine release, which is associated with rewarding function of VTA neurons.

In the frames of kinetic interpretation [9] the lognormal distribution of the interspike intervals (as observed in

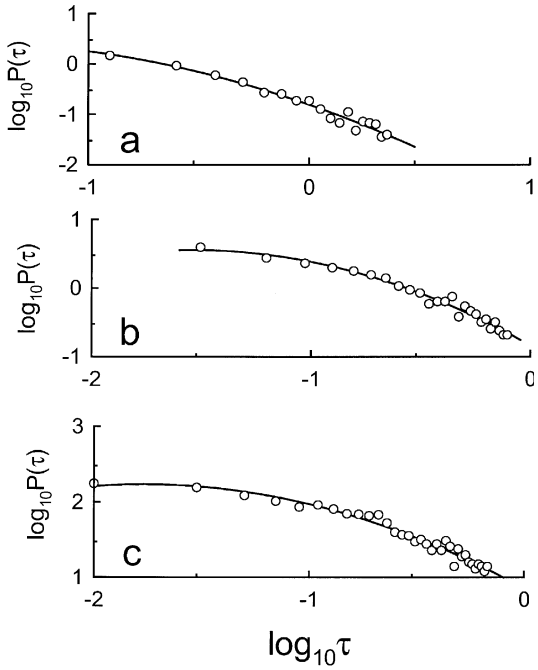


**Fig. 1.** Logarithm of probability density functions, $P(\tau)$, against logarithm of $\tau$. $P(\tau)$ were calculated using data from three dopaminergic neurons (Figs. 1a, b and c) of the FSL rats. Solid curves (the best fit) indicate lognormal distributions.

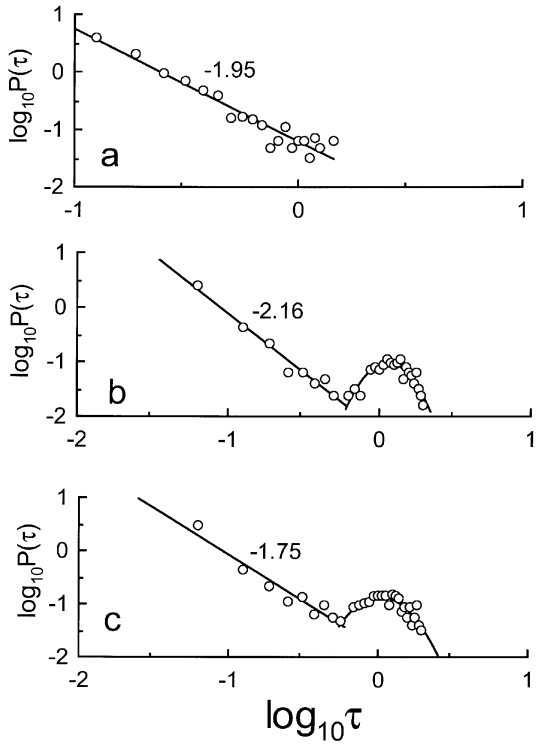


**Fig. 2.** Logarithm of probability density functions, $P(\tau)$, against logarithm of $\tau$. $P(\tau)$ were calculated using data from three dopaminergic neurons (Figs. 2a, b and c) of the rats from control (healthy) group. Solid straight lines (the best fit) indicate power-law distribution. Solid (bell shaped) curve is also drawn in Figures 2b and c to indicate a lognormal-like tail.

Fig. 1) has its origin in Gaussian distribution of the membrane activation thresholds. The power-law distribution observed for the healthy dopaminergic neurons (Fig. 2) can be interpreted as one produced by Boltzman distribution of the membrane activation thresholds. It means that short-range firing has purely kinetic nature (presumably related to the ion channels kinetics, see [9] and references therein). Therefore, in order to obtain information about system behavior one should turn to the long-range correlations, *i.e.* to multifractal analysis [12].

## 4 Long-range correlations

In reference [12] the long-range correlations in the spiking time-series of Red Nucleus were investigated using moments (structure functions) of order $p$

$$\langle \Delta T_r^p \rangle = \langle [T(n+r) - T(n)]^p \rangle \tag{1}$$

where $\Delta T_r$ indicates the temporal distance between the $(n+r)$th and $n$th neuron spike, and $\langle ... \rangle$ means average over the time-series. Case $r = 1$, corresponding to the interspike intervals, has been studied in previous section. In the present section we study general case of function $\Delta T_r$ with arbitrary $r$ (generalized interspike interval according to terminology accepted in [12]).

Figures 3a and b show, as an example, the moments of orders $p = 1, 2, ...7$ *versus* $r$ calculated for two cells: f11 (FSL rat # 1, cell # 1) and c11 (control rat # 1, cell # 1). Upper sets of the data correspond to higher value of order $p$. One can see that the data, like analogous data for Red Nucleus neurons (*cf.* [12]), exhibit a profound interval with scaling behavior

$$\langle \Delta T_r^p \rangle \sim r^{rH_p} \tag{2}$$

for $r > 10$. Analogous situation takes place also for other cells studied in the present experiment. Since the largest bursts in the signals consist of no more than 10 spikes this can be regarded as a long-range scaling.

Figures 4a and b show values of the generalized Hurst exponents $H_p$ (see (2)) for the FSL and for the control neurons. The solid straight lines indicate nonlinear dependence of $H_p$ on $p$

$$H_p = a + bp^{1/3}. \tag{3}$$

Such nonlinear dependence of $H_p$ on $p$ corresponds to so-called bi-lognormal distribution

$$P((\ln \tau)^2) \sim \exp - \left\{ \frac{[(\ln \tau)^2 - m]^2}{\sigma^2} \right\} \tag{4}$$

related to self-averaging phenomenon, see Appendix A. In order to check this directly several examples of probability density function of $(\ln \tau)^2$ (where $\tau = \Delta T_r$ with $r = 30$) were shown in Figure 5. The axes are chosen as $P((\ln \tau)^2)$ against $(\ln \tau)^2$ to check applicability of the bi-lognormal distribution (4) to these data. The solid parabolas (best fit) indicate the bi-lognormal distribution (4).

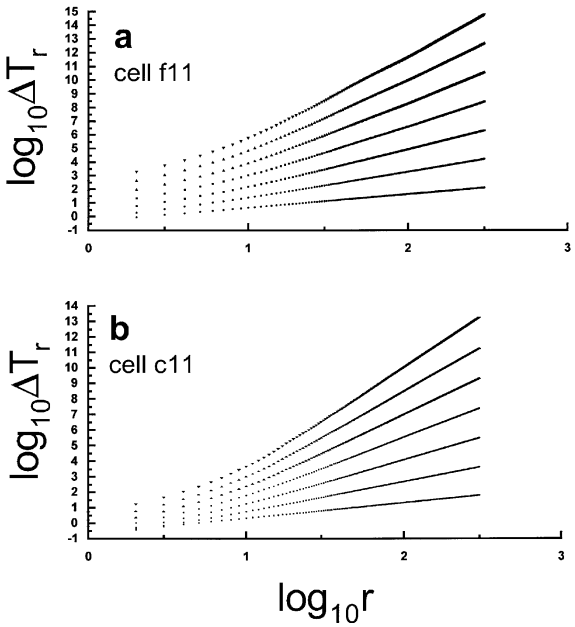


**Fig. 3.** Moments of $\Delta T_r$ *versus* $r$ in log-log scales for $p = 1, 2..., 7$ (upper sets of data correspond to higher values of $p$). Figure 3a shows data obtained for a FSL rat and Figure 3b shows data obtained for a rat from control group.

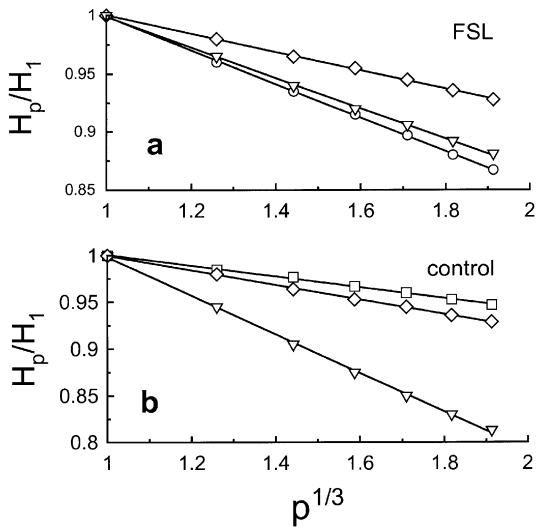


**Fig. 4.** $H_p$ *versus* $p^{1/3}$ for three FSL neurons (a), and for three control (healthy) neurons (b). The straight lines (the best fit) indicate nonlinear dependence (3).

It is interesting to compare this result to corresponding results obtained for Red Nucleus in [12]. Again, as for Red Nucleus, the probability distributions of the long-range generalized interspike intervals are of the same type for the FSL and for the control (healthy) neurons (at least in the probabilty tails). For the more simple Red Nucleus neurons we observe simple lognormal distribution of long-range $\Delta T_r$ (corresponding to linear dependence of $H_p$ on $p$ [12]), while for the dopaminergic neurons of VTA an intermediate self-averaging process (transforming the log-normality to bi-lognormality, see Appendix A) takes place.

It is possible that the origin of the lognormal-like behavior on the long ranges for the dopaminergic neurons is the same as for the Red Nucleus cells. However, much more complicated bursting activity of the dopaminergic neurons on the intermediate scales results in the self-averaging phenomenon.

It should be noted that the same self-averaging phenomenon is observed both for the FSL and for the healthy rats. Since rewarding function of VTA is suppressed for the FSL rats this phenomenon is independent on rewarding function of the VTA neurons. This observation, in particular, means that the specific system properties of VTA are not reduced to its rewarding function.

The authors are grateful to K.R. Sreenivasan and to P. Levin for cooperation and to the Machanaim Center (Jerusalem) for support. Referee's comments and suggestions were useful for this paper improvement.

## Appendix A

A natural modification of the Central Limit Theorem is related to a possibility of an intermediate self-averaging. Namely, the random variables $a_i$, which evolve the sum

$$a \sim \sum_i a_i \tag{A.1}$$

utilized in the Central Limit Theorem, can be self-organized in some clusters (bursts) in such a way that an averaging over each cluster is possible. If the whole system possesses also a self-similarity, then this intermediate averaging can result in significant modification of the tails of the probability distributions generated by the Central Limit Theorem. For the ergodic dynamical systems (where average over ensemble can be replaced by a time average) this phenomenon can be described in the most simple way, due to well known separation between so-called fast and slow motions. Indeed, let denote the time average as

$$\overline{a(t)} = \frac{1}{T}\int_0^T a(t')\mathrm{d}t'. \tag{A.2}$$

In the ergodic theorem one should take limit $T \to \infty$ in (A.2) to obtain corresponding ensemble average. However, the dynamical system can posses two types of motions: fast and slow. To eliminate the fast motion from consideration one can take an intermediate average (A.2) with $T$ much larger than characteristic times of the fast motion. If $T$ is still much smaller than characteristic times of the slow motions, then the new variable $\overline{a(t)}$ is still a function of time, but now it is already "slow" function of time.

Let us now take square power of equation (A.1)

$$a^2 \sim \sum_i a_i^2 + \sum_{i\neq j} a_i a_j$$

and let us take the intermediate average of this equation

$$\overline{a^2} \sim \sum_i \overline{a_i^2} + \sum_{i\neq j} \overline{a_i a_j}. \tag{A.3}$$

The crucial point of the whole consideration is that the statistical independence of the variables $a_i$ (a condition of the Central Limit Theorem) is *already* realized on the fast level, *i.e.* for intermediate average

$$\overline{a_i a_j} \simeq 0 \tag{A.4}$$

if $i \neq j$.

Then, we obtain from (A.3)

$$\overline{a^2} \sim \sum_i \overline{a_i^2}. \tag{A.5}$$

Let us introduce new variables

$$\overline{a^2} = A^2 \tag{A.6}$$

and

$$\overline{a_i^2} = A_i^2. \tag{A.7}$$

In these variables equation (A.5) can be written as

$$A^2 \sim \sum_i A_i^2. \tag{A.8}$$

Variables $A_i^2$ are statistically independent, *i.e.* for $i \neq j$

$$\left\langle A_i^2 A_j^2 \right\rangle = \left\langle A_i^2 \right\rangle \left\langle A_j^2 \right\rangle \tag{A.9}$$

where $\langle ... \rangle$ means average over infinite time period (or ensemble average).

Let us take the ensemble average $\langle ... \rangle$ over equation (A.8)

$$\left\langle A^2 \right\rangle \sim \sum_i \left\langle A_i^2 \right\rangle \tag{A.10}$$

and then subtract equation (A.10) from equation (A.8). Introducing new variables

$$x = A^2 - \left\langle A^2 \right\rangle \tag{A.11}$$

and

$$x_i = A_i^2 - \left\langle A_i^2 \right\rangle \tag{A.12}$$

we obtain

$$x \sim \sum_i x_i \tag{A.13}$$

where

$$\langle x_i x_j \rangle = 0 \tag{A.14}$$

for $i \neq j$. Then applying the Central Limit Theorem to the slow variables $x$ we obtain normal distribution of these slow variables, *i.e.*

$$P(A^2) = c \exp - \left\{ \frac{(A^2 - \langle A^2 \rangle)^2}{\sigma^2} \right\} \qquad \text{(A.15)}$$

or for variable $A$

$$P(A) = 2c|A| \exp - \left\{ \frac{(A^2 - \langle A^2 \rangle)^2}{\sigma^2} \right\}. \qquad \text{(A.16)}$$

Let us recall that from definition (A.6)

$$|A| = \sqrt{\overline{a^2}}. \qquad \text{(A.17)}$$

Thus, applying directly the Central Limit Theorem to variable $a$ (A.1) one obtains normal distribution for $a$. However, if there is good separation between fast and slow processes, then for variable $A$ (defined by (A.6) or (A.17)) one obtains probability distribution (A.16). The last distribution is approximately normal in a small vicinity of $\sqrt{\langle A^2 \rangle} = \sqrt{\langle a^2 \rangle}$, but for large deviation from the peak it exhibits behavior very different from normal distribution. Further we will call this new distribution bi-normal.

Appearance of the bi-normal distribution was shown above for the ergodic processes. It is clear, however, that the intermediate self-averaging phenomenon should take place for a wider class of random processes (in particular, for self-similar processes with clusterization on relatively small scales). Microscopically normal (Gaussian) processes affected by the intermediate self-averaging can result in the macroscopically bi-normal distributions. Since near its peak the bi-normal distribution behaves as a normal one, we should look on the tales in order to distinguish between the normal and the bi-normal situations.

Further, for *multiplicative* processes the microscopic *lognormal* distribution could result in the macroscopic *bi-lognormal* distribution. Multifractal properties of the log-normal distribution are described by linear dependence of generalized Hurst exponent $H_p$ on $p$ (see [9])

$$H_p = a + bp$$

whereas the multifractal properties of the bi-lognormal distribution are described by a nonlinear dependence of generalized Hurst exponent $H_p$ on $p$

$$H_p = a + bp^{1/3}. \qquad \text{(A.18)}$$

To obtain (A.18) one should estimate the scaling moments

$$\langle \Delta T_r^p \rangle \sim \int_0^\infty \Delta T_r^p \; P(\Delta T_r) \; \mathrm{d}\Delta T_r \sim r^{pH_p} \qquad \text{(A.19)}$$

with the bi-lognormal distribution

$$P((\ln \Delta T_r)^2) \sim \exp - \left\{ \frac{\left[ (\ln \Delta T_r)^2 - \langle (\ln \Delta T_r)^2 \rangle \right]^2}{\sigma^2} \right\}.$$

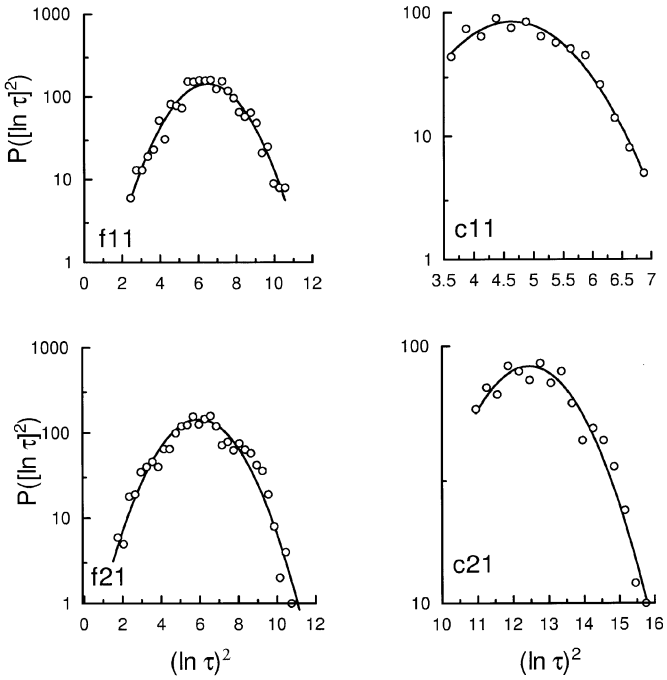


**Fig. 5.** Logarithm of probability density function $P([\ln \tau]^2)$, calculated for $\tau = \Delta T_r$ with $r = 30$, against $(\ln \tau)^2$. The solid parabolas (the best fit) are drawn to indicate bi-lognormal distribution (4).

This estimate can be produced using rather cumbersome saddle-point approximation, which is described in detail in [14] and results in equation (A.18) for generalized Hurst exponent $H_p$ from (A.19).

## References


1. C. Ivey, A.V. Apkarian, D.R. Chialvo, J. Neuroscience **79**, 1879 (1998)
2. D.R. Chiavlo, A. Longtin, J. Muautller-Gerking, Phys. Rev. E **55**, 1798 (1997)
3. R. Fakir, Phys. Rev. E **58**, 5175 (1998)
4. M. Di Mascio, G. Di Giovanni, V. Di Matte, E. Esposito, Lett. to Neuroscience **89**, 1003 (1999)
5. M. Di Mascio, G. Di Giovanni, V. Di Matteo, E. Esposito, Neuroscience **92**, 237 (1999)
6. J. Fing, B. Tirozzi, Phys. Rev. E **61**, 4207 (2000)
7. J.A. White, J.T. Rubinstein, A.R. Kay, Trends Neurosci. **23**, 131 (2000)
8. N. Hohn, A.N. Burkitt, Phys. Rev. E **63**, 031902 (2001)
9. A. Bershadskii, E. Dremencov, D. Fukayama, G. Yadid, Eur. Phys. J. B **24**, 409 (2001)
10. H.E. Plesser, Th. Geisel, Phys. Rev. E **63**, 031916 (2001)
11. C. van Vreeswijk, H. Sompolinsky, Science **274**, 1724 (2001)
12. A. Bershadskii, E. Dremencov, D. Fukayama, G. Yadid, Europhys. Lett. **58**, 306 (2002)
13. M.B. Carpeuter, J. Sutin, *Human Neuroanatomy* (Williams and Wilkins Co., Baltimore, 1983).
14. A. Bershadskii, Europhys. Lett. **53**, 716 (2001)